


## Strain-tuned magnetic properties in (Ga,Fe)Sb: First-principles study

Feng-Chun Pan(潘凤春), Xue-Ling Lin(林雪玲), and Xu-Ming Wang(王旭明)
**Citation:**Chin. Phys. B, 2021, 30 (**9**): 096105. DOI: 10.1088/1674-1056/ac0788
Journal homepage: http://cpb.iphy.ac.cn; http://iopscience.iop.org/cpb

**What follows is a list of articles you may be interested in**

---

## First neutron Bragg-edge imaging experimental results at CSNS

Jie Chen(陈洁), Zhijian Tan(谭志坚), Weiqiang Liu(刘玮强), Sihao Deng(邓司浩), Shengxiang Wang(王声翔), Liyi Wang(王立毅), Haibiao Zheng(郑海彪), Huaile Lu(卢怀乐), Feiran Shen(沈斐然), Jiazheng Hao(郝嘉政), Xiaojuan Zhou(周晓娟), Jianrong Zhou(周健荣), Zhijia Sun(孙志嘉), Lunhua He(何伦华), and Tianjiao Liang(梁天骄)
Chin. Phys. B, 2021, 30 (**9**): 096106. DOI: 10.1088/1674-1056/ac0da7

## Influence of helium on the evolution of irradiation-induced defects in tungsten: An object kinetic Monte Carlo simulation

Peng-Wei Hou(侯鹏伟), Yu-Hao Li(李宇浩), Zhong-Zhu Li(李中柱), Li-Fang Wang(王丽芳), Xingyu Gao(高兴誉), Hong-Bo Zhou(周洪波), Haifeng Song(宋海峰), and Guang-Hong Lu(吕广宏)
Chin. Phys. B, 2021, 30 (**8**): 086108. DOI: 10.1088/1674-1056/abf7ac

## Formation of nano-twinned 3C-SiC grains in Fe-implanted 6H-SiC after 1500-℃ annealing

Zheng Han(韩铮), Xu Wang(王旭), Jiao Wang(王娇), Qing Liao(廖庆), and Bingsheng Li(李炳生)
Chin. Phys. B, 2021, 30 (**8**): 086107. DOI: 10.1088/1674-1056/abff43

## Evolution of helium bubbles in nickel-based alloy by post-implantation annealing

Rui Zhu(朱睿), Qin Zhou(周钦), Li Shi(史力), Li-Bin Sun(孙立斌), Xin-Xin Wu(吴莘馨), Sha-Sha Lv(吕沙沙), and Zheng-Cao Li(李正操)
Chin. Phys. B, 2021, 30 (**8**): 086102. DOI: 10.1088/1674-1056/ac0783

## Controllable preparation and disorder-dependent photoluminescence of morphologically different $C_{60}$ microcrystals

Wen Cui(崔雯), De-Jun Li(李德军), Jin-Liang Guo(郭金良), Lang-Huan Zhao(赵琅嬛), Bing-Bing Liu(刘冰冰), and Shi-Shuai Sun(孙士帅)
Chin. Phys. B, 2021, 30 (**8**): 086101. DOI: 10.1088/1674-1056/ac0691

---

# Strain-tuned magnetic properties in (Ga,Fe)Sb: First-principles study*

Feng-Chun Pan(潘凤春), Xue-Ling Lin(林雪玲), and Xu-Ming Wang(王旭明)†

*School of Physics and Electronic-Electrical Engineering, Ningxia University, Yinchuan* 750021, *China*

(Received 2 April 2021; revised manuscript received 7 May 2021; accepted manuscript online 13 May 2021)

In view of the importance of enhancing ferromagnetic (FM) coupling in dilute magnetic semiconductors (DMSs), the effects of strain on the electronic structures and magnetic properties of (Ga,Fe)Sb were examined by a first-principles study. The results of the investigation indicate that $Fe_{Ga}$ substitution takes place in the low-spin state (LSS) with a total magnetic moment of $1\mu_B$ in the strain range of $-3\%$ to 0.5%, which transitions to the high-spin state (HSS) with a total magnetic moment of $5\mu_B$ as the strain changes from 0.6% to 3%. We attribute the changes in the amount and distribution of the total moment to the influence of the crystal field under different strains. The FM coupling is strongest under a strain of about 0.5%, but gradually becomes weaker with increasing compressive and tensile strains. The magnetic coupling mechanism is discussed in detail. Our results highlight the important contribution of strain to magnetic moment and FM interaction intensity, and present an interesting avenue for the future design of high Curie temperature ($T_C$) materials in the (Ga,Fe)Sb system.

**Keywords:** GaSb, Fe, ferromagnetism, strain

**PACS:** 61.72.−y, 71.15.Pd, 71.20.−b **DOI:** 10.1088/1674-1056/ac00a2

## 1. Introduction

In the field of spintronics, dilute magnetic semiconductors (DMSs) that simultaneously provide intrinsic ferromagnetism and semiconducting properties can be achieved by substituting cations in conventional semiconductors with transition metals (TMs) or rare-earth elements, which have attracted much attention in recent decades.[1–5] Among these semiconductors, the III–V GaSb-based DMSs have attracted a large amount of research interest because of their possible high $T_C$ values and intrinsic ferromagnetism,[6–15] which are critical in applications. Sato *et al.* theoretically predicted that the $T_C$ of Mn-doped GaSb would be proportional to the Mn concentration.[16] Indeed, Tu *et al.* experimentally confirmed that $T_C$ increased with increasing Fe concentration in GaSb:Fe, and found that $T_C$ can reach 340 K when the Fe amounts to 25%.[12–14] Therefore, increasing the dopant concentration is an effective approach to increase $T_C$. In order to further improve the TM concentration, unconventional preparation methods, such as high pressure and high temperature (HPHT) growth, should be used.[17,18] However, high TM concentrations imply an increasing probability of the second FM phase (such as MnSb),[19,20] which should be eliminated from the viewpoint of applications. Therefore, it is very necessary to seek other effective ways of achieving high $T_C$ and inherent ferromagnetism in TM-doped GaSb systems. More recently, many studies have indicated that strain can be used to modulate various physical properties.[21–26] Linpeng *et al.* highlighted the important contribution of strain to the relaxation and dephasing of acceptor-bound hole spins.[21] Strain can induce a transition from the semiconducting state to a metallic state in some bilayers.[23] It is interesting to note that the magnetocrystalline anisotropy in $(Ga_{0.8},Fe_{0.2})Sb$ exhibits a dependence on epitaxial strain and changes its sign from negative to positive when the strain is changed from tensile to compressive.[24] Furthermore, strain is commonly present at heterointerfaces and can easily be controlled by choosing a different substrate. Obviously, it is very significant to investigate the effects of strain on magnetic moment distribution and magnetic interactions in the GaSb:Fe system.

To clarify the influence of strain, in this article we systematically study the electronic structures and magnetic properties of the GaSb:Fe system under different strains using a first-principles approach. The results indicate that $Fe_{Ga}$ substitution takes place in the LSS with a total magnetic moment of $1\mu_B$ under strains in the range of $-3\%$ to 0.5%, which transitions to the HSS with a total moment of $5\mu_B$ as the strain changes from 0.6% to 3%. We attribute the changes to the size and distribution of the total moment to the influence of the crystal field under different strains. We find that the FM coupling is strongest under about 0.5% of tensile strain, which gradually weakens with increasing compressive and tensile strains. Our results highlight the important contribution of strain to magnetic moment and FM interaction intensity, and present an interesting avenue for the future design of high $T_C$ materials using the (Ga,Fe)Sb system.

*Project supported by the National Natural Science Foundation of China (Grant Nos. 11764032 and 11665018).

†Corresponding author. E-mail: wang_xm@126.com

© 2021 Chinese Physical Society and IOP Publishing Ltd 

## 2. Computational methods

The calculations are carried out according to spin-polarized density functional theory (DFT) and the local-density approximation (LDA) method of exchange–correlation parameterization, as implemented in the CASTEP package.[27,28] A cutoff energy of 380 eV is used for the plane-wave basis set, and the convergence criterion for self-consistent calculation is set to $1.0 \times 10^{-6}$ eV/atom. Brillouin zone sampling is performed using gamma-centered $3 \times 3 \times 3$ Monkhorst–Pack $k$-points.[29] The ion–electron interaction is described by the ultra-soft pseudopotential (USPP) method. In order to better describe the electronic structures of intrinsic GaSb, the Hubbard $U$ parameter has been employed to treat both Sb-3p and Ga-3d electrons. We tuned a number of the different parameters of $U$ to match the experimentally observed values of the band gap ($E_g$) and the lattice constants as far as possible, and we finally selected $U$ values of $U_{\text{Sb-3p}} = 3.0$ eV, $U_{\text{Ga-3d}} = 2.5$ eV. The larger $U_{\text{Sb-3p}}$ mainly stems from the fact that the band edge is dominated by the characteristics of Sb-3p, and is more effective at opening the gap of GaSb, which is similar to that of $TiO_2$.[30] With these parameters, the calculated values of $E_g = 0.809$ eV, $a_0 = b_0 = c_0 = 5.9116$ Å, are in good agreement with the experimental ones.[31] The relaxed structure of blende GaSb is shown in Fig. 1. In this article, the strain is defined as $\varepsilon\% = (a - a_0)/a_0$, where $a_0$ and $a$ are the unstrained and constrained lattice constants, respectively. For each deformed structure, all atoms are fully relaxed, with a fixed lattice constant.

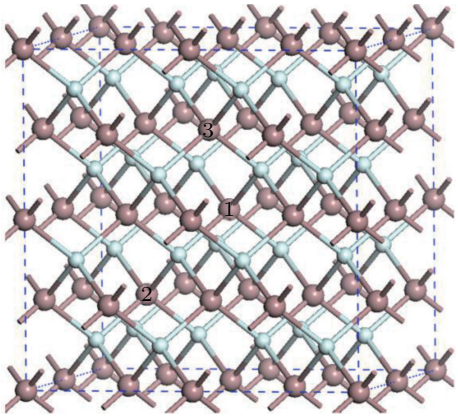



**Fig. 1.** The structure of GaSb; the big and small balls represent Ga and Sb atoms, respectively. Arabic numerals denote the sites of doped Fe.

## 3. Results and discussion

We first studied the effect of strain on the electronic structures and magnetic moment of a single-$Fe_{Ga}$-doped GaSb system. Our results indicate that the Fe is in the LSS and that the density of states (DOS) and the distribution of the magnetic moment are similar to those when the strain in the range of $-3\%$ to 0.5%. The total DOS (TDOS) and projected DOSs (PDOSs) at a strain of 0% are presented in Fig. 2. As shown in Fig. 2(a), the asymmetric electron occupation between the spin-up and spin-down states indicates that there is a magnetic moment in the system. The PDOSs in Figs. 2(b)–2(d) further clarify the source of the magnetic moment. For Fe-d electrons, the number of occupied spin-up electrons is more than that of occupied spin-down electrons, which can provide positive magnetic moments. However, for Sb (the nearest (N) and the next nearest (NN) to Fe)-s/p electrons, the number of occupied spin-down electrons is larger than that of occupied spin-up electrons. Therefore, the magnetic moments from Fe-d and the surrounding Sb-s/p electrons should be anti-parallel. As shown in Fig. 3(a), the distribution of spatial net spin electron density intuitively illustrates that the magnetic moments contributed by Fe-d and the surrounding Sb-s/p are, indeed, antiferromagnetic (AFM). Our results show that the total magnetic moment induced by $Fe_{Ga}$ is always $1\mu_B$ as the strain changes from $-3\%$ to 0.5%.

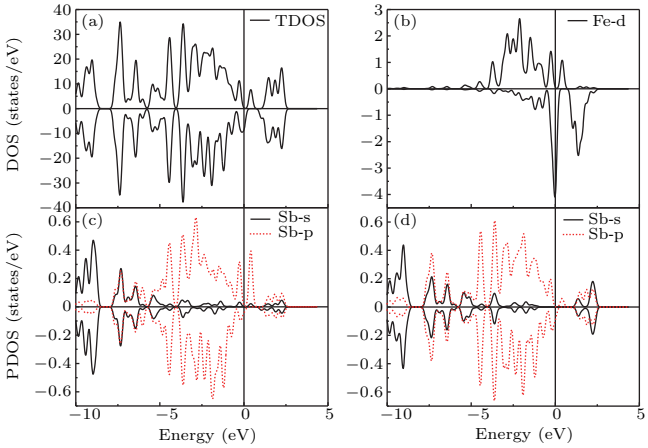



**Fig. 2.** Calculated TDOS (a) and PDOS for (b) Fe-d electrons, (c) Sb (N to Fe)-s/p electrons, and (d) Sb (NN to Fe)-s/p electrons in a single-$Fe_{Ga}$-doped GaSb system at a strain of 0%. The vertical lines denote the Fermi level. The TDOS and PDOS under strains of $-3\%$ to 0.5% have similar properties.

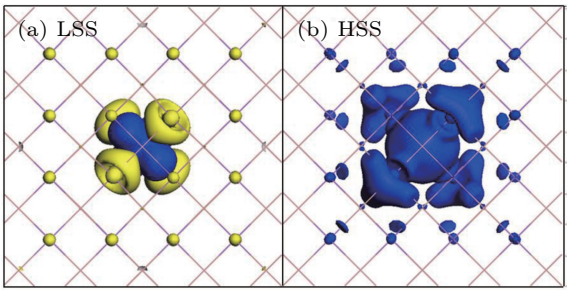



**Fig. 3.** The isosurface of spatial net spin electron density (a) in the one-$Fe_{Ga}$-doped GaSb system at a strain of 0%, (b) at a strain of 1%. The blue and yellow parts denote the spin-up and spin-down spatial net spin electron density, respectively. The isovalue is set to 0.01 $e$/Å$^3$.

When the strain increases to the range of 0.6% to 3%, the $Fe_{Ga}$ changes into the HSS and the total magnetic moment is $5\mu_B$. As shown in Fig. 4(a), the asymmetric TDOS means that a magnetic moment is present in the system; the PDOSs in Figs. 4(b)–4(d) present the contribution to the magnetic moment. It is obvious that the number of occupied spin-up electrons is larger than that of the occupied spin-down elec-

trons for Fe-d and the surrounding Sb-s/p electrons. Therefore, the magnetic moments contributed by Fe and ambient Sb should be parallel. The distribution of spatial net spin electron density as shown in Fig. 3(b) visually demonstrates that the magnetic moments are arranged in parallel. Obviously, the doped Fe induces spin-polarization of the GaSb host to a certain degree.[15] In addition, the distributions of the magnetic moment and the spin state are affected by strains. Compared with Figs. 2(b) and 4(b), it can be seen that the spin split of Fe-d under strains of $-3\%$ to 0.5% is smaller than that of Fe-d at strains of 0.6% to 3%, while the crystal field split in the range of $-3\%$ to 0.5% is larger than that at 0.6% to 3%, which indicates that the tightly surrounding Sb ions have great influence on the orbital energy level. Group theory will help us to further understand these results. The electron configuration of a single Fe atom is $[Ar]3d^6 4s^2$, which changes to $[Ar]3d^5$ for $Fe_{Ga}$ in the limit of the ionic GaSb crystal. Under the tetrahedral crystal field formed by the four surrounding Sb ions, the fivefold degenerate orbital of Fe-d will split into a doubly degenerate e orbital at a lower energy level and a triply degenerate $t_2$ orbital at a higher energy level. As illustrated in Fig. 5, the energy difference between $t_2$ and e at a strain of 0% is larger than that in the case of a 1% strain because of the stronger crystal field formed by the close Sb atoms, so that the orbital split energy between $t_2$ and e is greater than the electron pairing energy. In this situation, two spin-up electrons and two spin-down electrons occupy the e orbital and the remaining one electron occupies the $t_2$ orbital with spin-up, forming the electronic configuration $e^{\uparrow\uparrow\downarrow\downarrow}t_2^{\uparrow}$ (the arrows denote spin directions), which result in the LSS of Fe-d electrons, as shown in Fig. 5(a). Considering the covalent property of GaSb, from the calculated results for the magnetic moment contributed by Fe-d, we infer that about 1.36 electrons of the surrounding Sb-s/p jump back into the $t_2$ orbital with spin-up. Therefore, the electron configuration of Fe-d should be $e^{\uparrow\uparrow\downarrow\downarrow}t_2^{\uparrow\uparrow}$ (one short arrow denotes one electron and the large arrow denotes 1.36 electrons), which will induce $2.36\mu_B$. On the other hand, the Sb-s/p orbital's lost 1.36 electrons will lead to $-1.36\mu_B$. Therefore, the total magnetic moment is $1\mu_B$. With an increase in the tensile strain (1%, for example), the orbital split energy is smaller than the electron pairing energy because of the weaker crystal field formed by loose Sb atoms. In the limit of ionic crystal, five Fe-d electrons occupy the e and $t_2$ orbitals with the same spin orientation; the electron configuration is $e^{\uparrow\uparrow}t_2^{\uparrow\uparrow\uparrow}$, which leads to the HSS, as shown in Fig. 5(b). However, the covalent property of GaSb indicates that some Sb-s/p electrons will jump back to Fe-d orbitals. Because the spin-up orbital of Fe-d is fully occupied, only spin-down electrons of Sb-s/p can jump back to the Fe-d orbital. Further analysis indicates that about 1.40 electrons with spin-down jump back into the Fe-d orbital because of the covalent character of GaSb, which results in $3.60\mu_B$ for Fe-d and $1.40\mu_B$ for Sb-s/p. Therefore, the total magnetic moment at a strain of 1% is $5\mu_B$.

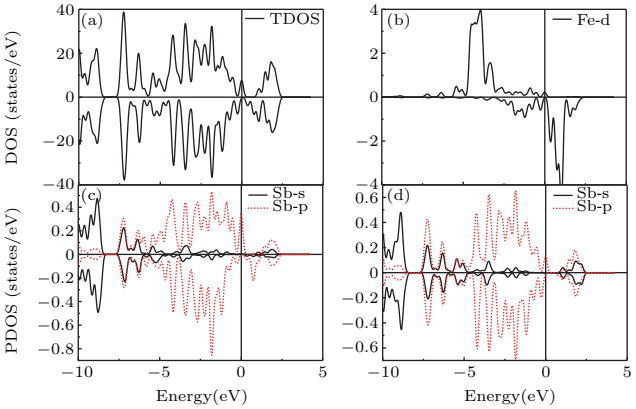



**Fig. 4.** Calculated TDOS (a) and PDOS for (b) Fe-d electrons, (c) Sb (N to Fe)-s/p electrons, and (d) Sb (NN to Fe)-s/p electrons in a single-$Fe_{Ga}$-doped GaSb system at a strain of 1%. The vertical lines denote the Fermi level. The TDOS and PDOS under strains of 0.6% to 3% have similar properties.

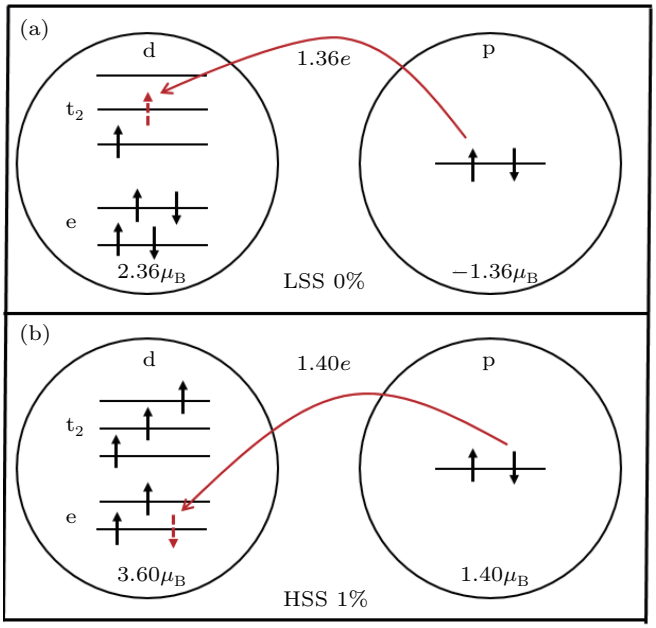



**Fig. 5.** Diagrammatic sketch of the magnetic moment when (a) Fe is in the LSS at a strain of 0%, and when (b) Fe is in the HSS at a strain of 1%.

The results of the study indicate that the total magnetic moment remains constant in the LSS or the HSS, but that the partial magnetic moment changes with strain, as shown in Fig. 6. In the range of $-3\%$ to 0.5%, the portion contributed by Fe is slightly enlarged and the portion contributed by Sb is slightly reduced with increasing strain. When the strain is 0.6%, the magnetic moment due to Fe sharply increases to $3.59\mu_B$, which indicates that the spin state of Fe changes to the HSS. Meanwhile, the portion due to Sb also suddenly increases. It is obvious that the portions due to Fe and Sb are basically unchanged as the strain changes from 0.6% to 3%.

In order to investigate the magnetic interactions, two Fe atoms are doped into a 64-atom GaSb supercell, located at the 1,2 sites (denoted as SI, in which the two Fe atoms are N) with a small separation and at the 2,3 sites (denoted as SII, in which

the two Fe atoms are NN) with a larger separation, as shown in Fig. 1, respectively. The magnetic coupling can be judged by the total energy difference between the FM and AFM phases ($\Delta E = E_{\rm AFM} - E_{\rm FM}$). The FM and AFM phases are defined by aligning the magnetic moment orientations of the two Fe atoms parallel or anti-parallel to each other. Furthermore, the FM coupling strength can be estimated by $T_{\rm C} = \frac{2\Delta E}{3k_{\rm B}x}$ according to mean-field theory,[16,32] where $k_{\rm B}$ is the Boltzmann constant, and $x\%$ is the doping concentration of Fe ($x\% = 6.25\%$ in this article).

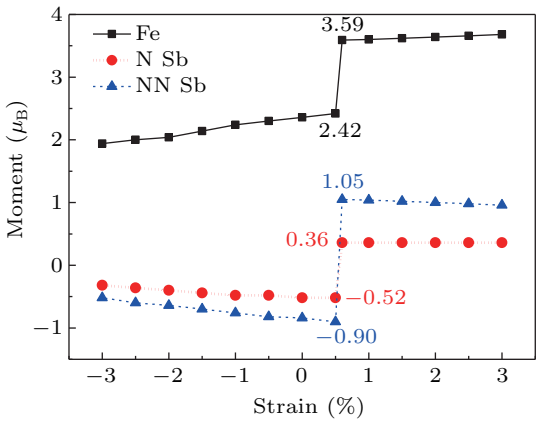



**Fig. 6.** The magnetic moment distribution with varying strain.

As shown in Fig. 7, the $T_{\rm C}$ values for SI and SII gradually increase with decreasing compressive strains in the range of −3% to 0.5%, and reach maxima of 311.8 K and 202.5 K at a strain of 0.5%, respectively, which decrease sharply as the strain increases to 0.6% and then continue to decrease with increasing strain. The maximum of 311.8 K for SI is close to the value of 336 K in (Ga,Mn)Sb with same doping concentration as estimated by mean-field theory.[11] Moreover, $T_{\rm C}$ decreases dramatically with an increasing distance between Fe atoms when the strain in the range of −3% to 0.5%, while the decreasing amplitude of $T_{\rm C}$ at strains of 0.6% to 3% is not so obvious. Comparing Figs. 6 and 7, it is inevitable that the critical value of the FM coupling strength is consistent with that of the Fe spin state. It is interesting to note that in the range of −3% to 3%, the FM coupling is always preferred. From the point of view of FM coupling intensity, the magnetic interaction is strongest at a strain of 0.5%.

Several different coupling mechanisms are responsible for the magnetic coupling properties in DMSs, which can lead to ferromagnetism or anti-ferromagnetism, and are very important to help us to understand the physical scenarios. We will then shed light on the FM interaction mechanism hidden in the GaSb:Fe system under different strains. For the LSS, as shown in Fig. 2, near the Fermi level, the spin-up and spin-down states are both occupied for Fe-d (Fig. 2(b)), which are located in the band-gap of GaSb. The characteristics of such PDOS structures are schematically depicted in Fig. 8(a). Obviously, under these conditions, Fe-d electrons can directly jump into another Fe-d orbital with the same spin orientation and vice versa, which results in FM coupling, as illustrated in Fig. 8(a). The FM coupling induced by the electron exchange of Fe-d–Fe-d is a double exchange mechanism,[33] which can be very strong over a short range.[4] As shown in Fig. 7, for the LSS in the range of −3% to 0.5%, the $T_{\rm C}$ of SI are higher than those of SII, which proves that the double-exchange model plays a key role in the FM interaction between two Fe atoms. However, for the HSS, as shown in Fig. 4, the larger spin-splitting energy pushes the spin-up states of Fe into a deeper level, which are then mixed with the extended and partially occupied spin-up states of Sb-p, as schematically shown in Fig. 8(b). Therefore, Fe-d electrons can couple with other Fe-d electrons through the Sb-p orbital, which can also lead to a FM interaction. The FM coupling between Fe-d electrons through Sb-p takes place via p–d exchange,[34,35] which is relatively weak, but works over a longer range.[4] As shown in Fig. 7, for the HSS in the range of 0.6 to 3%, the differences of $T_{\rm C}$ between SI and SII are not obvious, which is in agreement with the characteristic of p–d exchange. In

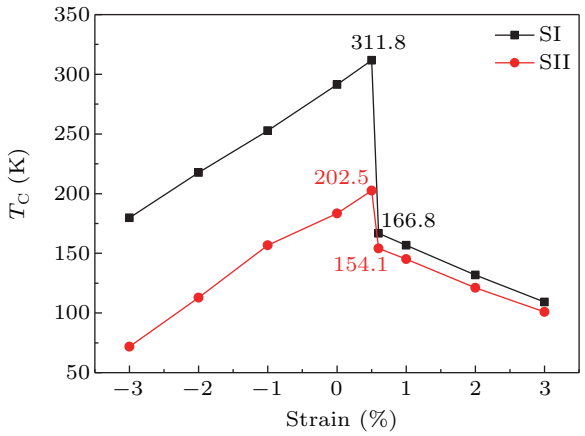



**Fig. 7.** The estimated $T_{\rm C}$ under different strains for SI and SII, respectively.

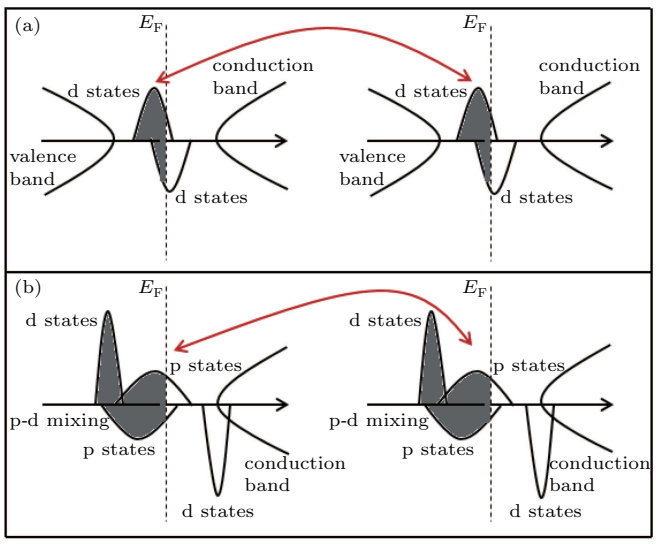



**Fig. 8.** Schematic diagrams of (a) double-exchange for the LSS at a strain of 0% and (b) p–d exchange for HSS at a strain of 1%. Dotted lines and shaded regions denote the Fermi level and occupied states, respectively.

fact, there is competition between double exchange and p–d exchange for (Ga,Fe)Sb under different strains, as presented in the (Zn,Mn,Li)Se system reported by Zhu *et al.*[36] In the range of $-3\%$ to 0.5%, the double exchange is dominant, while in the range of 0.6% to 3%, the p–d exchange plays a key role.

## 4. Conclusion

The effect of strain on the electronic structures and magnetic properties of (Ga,Fe)Sb have been studied using a first-principles calculation. The results of the investigation indicate that $Fe_{Ga}$ substitution takes place in the LSS with a total magnetic moment of $1\mu_B$ under strains in the range of $-3\%$ to 0.5%, which transition to the HSS with a moment of $5\mu_B$ as the strain changes from 0.6% to 3%. We attribute the changes in the size and distribution of the total moment to the influence of the crystal field under different strains. The FM coupling is strongest at a strain of about 0.5%, and gradually becomes weaker with increasing compressive and tensile strains. The magnetic coupling mechanism can be explained by the double exchange model in the range of $-3\%$ to 0.5%, and by p–d exchange model in the range of 0.6% to 3%. Our results highlight the important contribution of strain to magnetic moments and FM interaction intensity, and present an interesting avenue for the future design of high $T_C$ materials using the (Ga,Fe)Sb system.

## References


[1] Ohno H 1998 *Science* **281** 951
[2] Dietl T, Ohno H, Matsukura F, Cibert J and Ferrand D 2000 *Science* **287** 1019
[3] Dietl T 2010 *Nat. Mater.* **9** 965
[4] Sato K, Bergqvist L, Kudrnovský J, Dederichs P H, Eriksson O, Turek I, Sanyal B, Bouzerar G, Katryama-Yoshida H, Dinh V A, Fukushima T, Kizaki H and Zeller R 2010 *Rev. Mod. Phys.* **82** 1633
[5] Dietl T and Ohno H 2014 *Rev. Mod. Phys.* **86** 187
[6] You J, Gu B, Maekawa S and Su G 2020 *Phys. Rev. B* **102** 094432
[7] Takeda T, Suzuki M, Anh L D, Thanh Tu N, Schmitt T, Yoshida S, Sakano M, Ishizaka K, Takeda Y, Fujimori S, Seki M, Tabata H, Fujimori A, Strocov V, Tanaka M and Kobayashi M 2020 *Phys. Rev. B* **101** 155142
[8] Takeda T, Sakamoto S, Araki K, Fujisawa Y, Anh L D, Thanh Tu N, Takeda Y, Fujimori S, Fujimori A, Tanaka M and Kobayashi M 2020 *Phys. Rev. B* **102** 245203
[9] Tu N T, Hai P N, Anh L D and Tanaka M 2015 *Phys. Rev. B* **92** 144403
[10] Goel S, Anh L D, Tu N, Ohya S and Tanaka M 2019 *Rhys. Rev. Materials* **3** 084417
[11] Seña N, Dussan A, Fesa F, Castaña E and González-Hernández R 2016 *J. Appl. Phys.* **120** 051704
[12] Tu N T, Hai P N, Anh L D and Tanaka M 2014 *Appl. Phys. Lett.* **105** 132402
[13] Tu N T, Hai P N, Anh L D and Tanaka M 2015 *Phys. Rev. B* **92** 144403
[14] Tu N T, Hai P N, Anh L D and Tanaka M 2016 *Appl. Phys. Lett.* **108** 192401
[15] Zhang P, Kim Y H and Wei S H 2019 *Phys. Rev. Appl.* **11** 054058
[16] Sato K, Dederichs P H, Datayama-Yoshida H and Kudrnovský J 2004 *J. Phys.: Condens. Matter* **16** S5491
[17] Kondrin M V, Gizatullin V R, Popova S V, Lyapin A G, Brazhkin V V, V. Ivanov V Y, Pronin A A, Lebed Y B and Sadykov R A 2011 *J. Phys.: Condens. Matter* **23** 446001
[18] Ganesan K, Pendyala N B, Koteswara Rao K S R, Venkataraman V and Bhat H L 2010 *Semicond. Sci. Technol.* **25** 105003
[19] Abe E, Matsukura F, Yasuda H, Ohno Y and Ohno H 2000 *Physica E* **7** 981
[20] Boishin G, Sullivan J and Whitman L 2005 *Phys. Rev. B* **71** 193307
[21] Linpeng X, Karin T, Durnev M V, Glazov M M, Schott R, Wieck A D, Ludwig A and Fu K C 2021 *Phys. Rev. B* **103** 115412
[22] Patel K, Prosandeev S, Xu B, Xu C and Bellaiche L 2021 *Phys. Rev. B* **103** 094103
[23] Zhong H, Xiong W, Lv P, Yu J and Yuan S 2021 *Phys. Rev. B* **103** 085124
[24] Goel S, Anh L D, Ohya S and Tanaka M 2019 *Phys. Rev. B* **99** 014431
[25] Rawat K, Fong D D and Aidhy D S 2021 *J. Appl. Phys.* **129** 095301
[26] Breev I, Poshakinskiy A, Yakovleva V, Nagalyuk S, Mokhov E, Hübner R, Astakhov C, Baranov P and Anisimov A 2021 *Appl. Phys. Lett.* **118** 084003
[27] Hohenberg P and Kohn W 1964 *Phys. Rev.* **136** B864
[28] http://www.castep.org/CASTEP/ReferencingAndLogo.
[29] Pack D and Monkhorst H J 1977 *Phys. Rev. B* **16** 1748
[30] Orhan O and O'Regan D 2020 *Phys. Rev. B* **101** 245137
[31] Straumanis M and Kim C 1965 *J. Appl. Phys.* **36** 3822
[32] Sato K, Dederics P and Katayama-Yoshida H 2003 *Europhys. Lett.* **61** 403
[33] Zener C 1951 *Phys. Rev.* **82** 403
[34] Zener C 1951 *Phys. Rev.* **81** 440
[35] Dietl T, Ohno H, Matsukura F, Cibert J and Ferrand D 2000 *Science* **287** 1019
[36] Zhu Y, Liu T, Zhang X, Pan Y, Wei X, Ma C, Shi D and Fan J 2017 *Phys. Lett. A* **381** 1169